

NAVIGATION FOR VERTICAL PRECISION LANDING BASED ON OPTICAL TRACKING OF A SPATIAL RETROREFLECTIVE MARKER ARRAY

P. Hartmann*, C. Ben*, D. Moormann *

* Institute of Flight System Dynamics, RWTH Aachen University, Germany

Keywords: *Optical Tracking, Precision Landing, UAV*

Abstract

In this contribution the design and implementation of a navigation system using an optical tracking system for vertical precision landing on a small mobile platform is presented. The tracking system, designed to fulfil challenging project requirements regarding accuracy and reliability, is based on a spatial array of retroreflective flat markers.

A series of measurements focussing in particular on influence of distance and perspective of the camera relative to the marker array is carried out. Results are discussed with respect to the specific landing task requirements.

The concept proves the general suitability for this task. Besides some minor drawbacks regarding limitations in camera perspectives, the overall accuracy, in particular dependent on the distance between vehicle and landing platform, match well the landing requirements.

1 Introduction

Within the ANCHORS¹ project, which is part of the French-German “Research for Civil Security” programme and co-funded by the German Federal Ministry of Education and Research, a system for autonomous exploration of large-area catastrophes involving radioactive hazards like nuclear reactor incidents is developed. During the Fukushima Daiichi nuclear disaster in 2011, for the first time unmanned aerial vehicles (UAVs) have been used by

rescue forces to support radiological monitoring and investigate rubble areas with a high radiation risk to humans. The UAV application was successful but limited to short times of operation. [01]

The ANCHORS system is designed to operate in the case of comparable scenarios and consists of several ground and aerial robots. Fig. 1 shows a larger ground robot, called mobile transport system (MTS) that provides a base station for a swarm of several small multicopter UAVs as well as small unmanned ground vehicles.



Fig. 1: Mobile transport system with landing platform and recharging contacts²

¹ UAV Assisted Ad Hoc Networks for Crisis Management and Hostile Environment Sensing

² Image source: SGE Spezialgeräteentwicklung GmbH, Kerntechnische Hilfsdienst GmbH

To ensure the required availability of the overall ANCHORS system within the hazard area in combination with the limited range of multicopters, the mobile transport system is used to transport the multicopters into the incident-area. To achieve long-term operation of up to 100 hours, the UAVs are recharged and decontaminated on board the MTS. Since no human interaction is possible within the hazard area, an autonomous precision take-off and landing on a small platform (Fig. 1 bottom left) is necessary. The electrical charging contacts (Fig. 1 bottom right) and the decontamination equipment require a positioning within a few centimetres.

To meet the challenging requirements on navigation accuracy, an optical tracking setup is proposed. Reliability and robustness is improved by extending the concept of flat fiducial multi-marker arrays to a spatial marker array. Furthermore, the markers are provided with a retroreflective coating to enhance contrast and visibility in varying light environments. Since the overall ANCHORS system is required to have an operational availability of 95 %, the optical navigation system has to be capable to robustly operate under various light conditions at day and night time.

In this contribution a system design and implementation for the optical navigation is presented. A measurement series is carried out to evaluate the position estimation accuracy of the entire system. Especially dependencies of distance to the tracking reference object and of camera's perspective are investigated.

2 Tracking of small unmanned aerial vehicles

The term "tracking" in general denotes the process of locating a movable object in real time applications. In this general sense, tracking is not limited to the context of unmanned aerial vehicles. There are rather many other applications which make use of tracking technologies.

Applications include Robotics [02], motion capture or augmented reality installations [03]. Besides many others, especially optical tracking technologies have gained

importance in context of these applications. Thus a variety of optical tracking technologies has been developed apart from the UAV topic.

Tracking is one of the central challenges within UAV operation. For small UAVs, tracking is typically managed by using a global navigation satellite system (GNSS) in conjunction with an inertial measurement unit (IMU). As the absolute position accuracy in this setup depends on the GNSS, it is not sufficient for precision landing alone. Therefore an optical tracking method is proposed to augment the UAVs navigation system during landing.

The commonality amongst all optical tracking methods is the estimation of the relative position or pose³ between one or more cameras and a visible reference object by extracting features out of the camera images.

The tracked object can be identical or attached to the reference object and is tracked relative to a fixed camera (outside-in tracking) or the position of a movable camera is tracked relative to a fixed reference object (inside-out tracking) [04]. The reference object can be realized as a fiducial marker or as set of natural features of the tracked object or of the environment. Tracking with use of natural features is more difficult than with use of fiducial markers [05]. As our problem, landing on a mobile platform, allows the use of fiducial markers, we concentrate on tracking with use of them.

There are lots of different types of tracking methods with different types of fiducial markers. For augmented reality applications, flat square high-contrast patterned markers are widely used [03][06]. These methods are not very demanding in terms of computational resources but lack robustness. Their accuracy is depended on viewing angles [07], they do not work in dark environments and a partly covered marker often interrupts tracking. Some of the drawbacks can be compensated by the use of planar arrays of flat markers. Nevertheless, common-mode misdetection of markers, for example due to bright light sources like sunlight, is still a problem with planar arrays.

³ Pose: Position and Orientation

In robotics and motion capture applications systems with multiple simple shaped markers, like balls or points, are widely used. The perceptibility of such markers is often improved by the use of markers which are coloured unique within their environment [08] or by passive [09] or active visible or infrared illumination [10]. For outdoor environments [10] states, that artificial marker illumination cannot compete with light intensity provided by full sunshine and therefore the outdoor usage can be difficult. Passively illuminated markers, in most cases assisted by retroreflective marker coatings, are utilized for indoor UAV tracking [09]. Using this method, the *Flying Machine Arena* (FMA) provides very precise and robust tracking for multiple UAVs in a large-volume indoor environment [11]. The FMA makes use of up to 20 high resolution cameras. Tracking concepts like the one applied within the *Flying Machine Arena* are not suitable for the outdoor landing situation within the ANCHORS project.

3 Concept for robust pose estimation

To obtain an ideal tradeoff between system complexity and reliable accuracy we propose a new variant for optical pose estimation.

3.1 System design

The project requires fulfilling several features on the tracking system. Among these are the ability to track a number of UAVs at the same time and to operate outdoors during day- and nighttime. Concerning accuracy, the landing base fixed onto the mobile transport system defines a suitable minimum. The landing base is able to compensate position deviation up to 150 mm (see fig. 1, bottom row). The position error by the tracking system should be significantly smaller.

To meet the requirements, an inside-out tracking setup is applied. The concept of a flat array of square fiducial markers is extended to a spatial array of markers. The single markers are provided with a retroreflective coating to enhance contrast and visibility in varying light environments. The reference object, the array, is fixed to the mobile transport system and the

camera including processing peripheries is mounted on board the UAV. Therefore, no real time data link between MTS and UAV is necessary. Furthermore the tracking system cannot be busy; the reference object can be used by multiple UAVs without interference.

The spatial array of markers has several advantages compared to planar arrays. As long as the array is in the cameras field of view, for most perspectives the images include more than one marker. Each marker detection delivers complete pose estimation, because the single-marker poses relative to the array are known to the system. Due to the fact that markers are rotated against each other, the single-marker perspective is varying within a camera frame. The possibility to see at least one marker in a well-conditioned way is raised, common-mode reflections are suppressed. Additionally, if more than one marker is in field of view, the tracking becomes less vulnerable against partly covered markers. Different sized markers can extend the operational range between array and camera. All bright areas of the markers are substituted by a retroreflective coating and are illuminated by a light source mounted directly next to the camera on board the UAV. The desired reflection hits the corresponding light emitting UAV only. Other UAV's tracking systems are not disturbed.

3.2 Implementation

The payload margin of the ANCHORS UAV is limited. Thus, the single board computer (SBC) *Overo IronSTORM COM*⁴ with very small dimensions and a Cortex-A8 processor core was chosen. The associated camera, *Caspa VL*, has a resolution of 752x480 and uses a global shutter system for undistorted imaging of motions. The maximum frame rate is 60 fps and exposure is adjusted automatically. The lens is of fixed focus and fixed focal length type. The lens distorts the image noticeable, so an intrinsic calibration of the camera was done with the help of *Camera Calibration Toolbox for Matlab*⁵. The camera's interface allows direct access to the computer's memory. So images can get into

⁴ <http://www.gumstix.com>

⁵ http://www.vision.caltech.edu/bouguetj/calib_doc/

memory and being directly processed by the marker detection software without adding load to the processor.

For single-marker detection the *ARToolkitPlus* (ARTK+) [12] software is used. ARTK+ is able to detect and distinguish between up to 4096 different square markers. It is optimized to run on systems with low processing power. Thus, the chosen Cortex-A8 core system is an adequate target platform. To calculate markers' poses, the toolkit has to be aware of the dimensions of all used markers. The resulting poses are outputted in form of 4x4-transformation matrices (M_{c,m_i}) stating the pose for each individual marker.

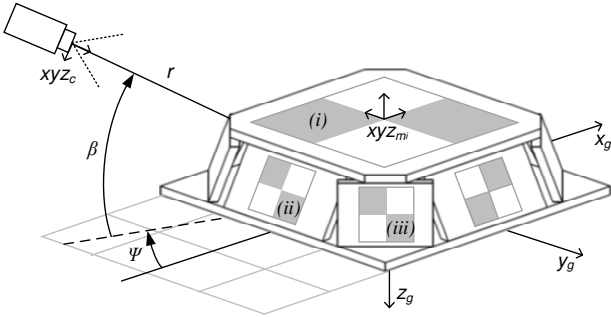


Fig. 2: Spatial marker array and camera perspective

The realized array design has overall dimensions of 500x500x126 mm and thus fits on top of the MTS. The array's coordinate system is identical to the global coordinate system for the performed measurements and shown in figure 2. Each marker has an own coordinate system fixed to each marker plane. Bright marker areas are coated with *Scotchlite High Gain 7610* film. This film has a homogenous retroreflective surface. Without external illumination its appearance is light grey, so without illumination the contrast between dark and bright areas is reduced compared to simple white bright areas (compare fig. 3 upper left). Illumination is provided by a LED with warm-white colour temperature and a maximum power of 1 W.

The array consists of 9 different markers, one large and eight smaller ones. The large marker on top measures 280 mm (*i*, compare fig. 2), four small marker measure 90 mm (*ii*), another four measure 77 mm (*iii*) edge length. The small markers are uniformly

rotated around the vertical axis of the array (45° steps), tilt angles against horizontal plane alternate between 60° (*ii*) and 70° (*iii*). The arrangement allows an omnidirectional usage.

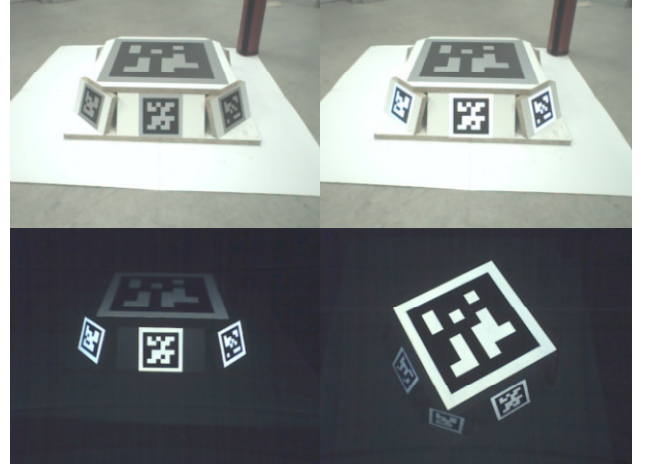


Fig. 3: Marker array at different lighting conditions: upper left: daylight, illumination non-active, upper right: daylight, illumination active, bottom: darkness, illumination active

For each marker, the pose relative to the array coordinate system is given in a 4x4 pose matrix $M_{m_i,g}$ expressed in homogeneous coordinates. With a given detection of one marker by the ARTK+ software the transformation from camera to global coordinate system based on detection of marker *i* is given by:

$$(M_{g,c})_i = (M_{c,m_i} \cdot M_{m_i,g})^{-1} \quad (1)$$

The rotational part of this estimation is not as precise as the UAV's own orientation estimation by an IMU system. Thus, this part is neglected and only the position estimation is used for the UAV's navigation. As equation 1 shows, a position estimate based on each recognised marker exists. If an image comes up with more than one position estimate, outliers can be recognized and rejected. For this detection, the arithmetic average of the positions is calculated. After that, the distances from each marker to this average position are compared to the distance from the marker array to the average position. If a single distance marker-to-average is bigger than 15% of the distance average-to-array, then the image's estimations are rejected. Otherwise, the average position is kept as

position estimate. Estimates by images that include only one marker cannot be improved by this sanity check.

4 Evaluation of accuracy

To evaluate the achievable accuracy of the implemented tracking system, a series of measurements was carried out. By variation of the camera's distance r , elevation β and azimuth Ψ (see fig. 2) relative to the array's origin of ordinates, several relative positions were arranged. The estimated positions were compared to the predefined positions.

4.1 Measurement setup

To vary elevation and distance the camera was mounted in different fixed positions while the marker array stayed in one position. The azimuth was varied by rotating the array. The reference position could be measured externally with an accuracy of roughly 10 mm.

The viewing direction of the camera was maintained to be in direction of the array. Previous test showed, that with more ambient light available, the position estimates gets slightly more accurate. Detection rate of markers per image is slightly increased. So, for the series of measurements the worst condition, complete darkness, was chosen. Fig. 3 shows different lightning conditions: the right upper corner shows the array with ambient light and illumination switched on, the bottom row shows two situations without ambient light. Note that the contrast of markers depends only slightly on the ambient light condition. Therefore, accuracy only differs slightly with ambient light condition.

At all camera positions 100 images were grabbed and processed, all marker detections were recorded. Due to image noise, processing results are not the same for one position. This leads to noise in the estimated positions. This noise is taken into account by sampling 100 images per position. Table 1 shows, which positions were investigated. The table is not filled completely because of limitations in height of measurement room. For each table item, azimuths 0° , 10° , ... 80° were measured. All azimuth angles of 90° and above are

equivalent to azimuth angles from 0° to 90° because the array has two rectangular planes of symmetry.

	$\beta = 10^\circ$	$\beta = 30^\circ$	$\beta = 50^\circ$	$\beta = 70^\circ$
$r = 1.0 \text{ m}$	(a)	(b)	(c)	(d)
$r = 1.5 \text{ m}$	(e)	(f)	(g)	-
$r = 2.5 \text{ m}$	(h)	(i)	-	-

Tab. 1: Measurement points

4.2 Results

Before detailed results on accuracy are presented, some general results are summarized. The measurement series involved 81 different camera positions. For nine positions no position estimate could be provided. These nine positions all belong to a distance of 2.5 m and an elevation of 10° (compare tab. 1, (h)). Due to the flat viewing angle, the larger marker could not be detected and the small markers appeared too small on images belonging to distances of 2.5 m. Thus, all measurements (h) are neglected in the following results.

Within the 72 remaining positions 7200 images had been taken and analysed. In average 1.69 markers were detected per image. The value seems to be a bit low compared with the average markers in the camera's field of view. This indicates that not every visible marker is detected. On 510 images no marker could be detected. 6612 images led to a position estimation that passed the sanity check. 78 images led to position estimates that did not pass the sanity check described in chapter 3.2. The exact sanity check margin (here 15%) has little effect on the activity of the sanity check. The excluded estimations failed the check far beyond this threshold value.

The image processing speed of the system showed to be slower than expected. While no or only one marker is in the camera's field of view, the processing could be performed with full camera frame rate of 60 fps. As soon as two or more markers appeared, the analysis took significant longer processing times. To prevent the system from varying the frame rate all the time, the frame rate was limited to 10 fps for the analysis.

For the detailed analysis, the 100 images for each position were summed up. All position estimations that went through the sanity check were compared to the reference position and absolute position differences were calculated. Hereafter, the term error denotes this absolute position differences. The mean value and standard deviations of errors for each position is given in figure 4. The mean error is marked with black crosses, standard deviation by blue error bars. Please note the logarithmic error-axis. The plot is grouped for each combination of distance and elevation. The groups are labelled (a) to (i) consistent to table 1. Each group includes mean error and standard deviation for all azimuth angles investigated. Azimuth angles of $0^\circ, \dots, 80^\circ$ are plotted from left to right within each group.

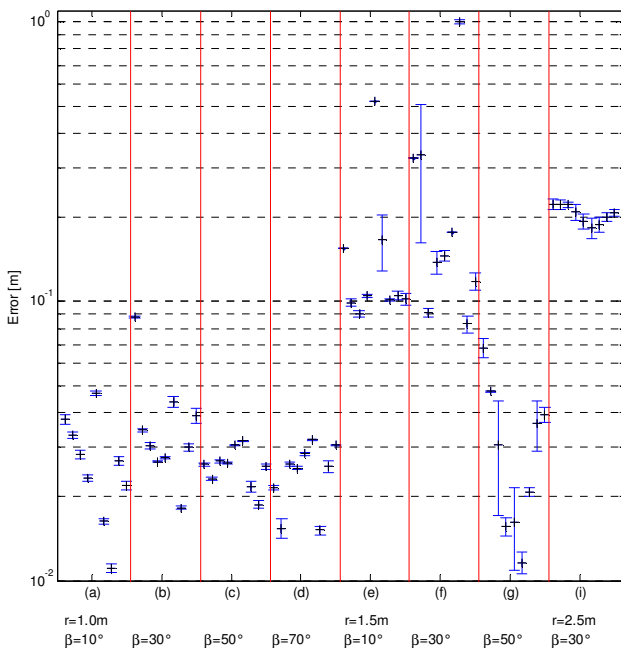


Fig. 4: Mean and standard deviation of errors in estimated positions; aggregation according to table 1

Within the groups (a)-(d), belonging to a distance of 1.0 m, all position estimations show very little errors. Neglecting one exception, all errors are below 50 mm. All standard deviations are small compared to the absolute errors. The elevation seems to have little influence on the mean of errors. With some exceptions the estimations are based on detections of the smaller markers. Dependency on azimuth angle is discussed below.

Group (i), belonging to a distance of 2.5 m, shows a decreasing accuracy reporting errors in range of 200 mm. All estimations are based on the larger marker alone. The smaller markers could not be detected at this distance, which is why within group (h) no estimation could be provided.

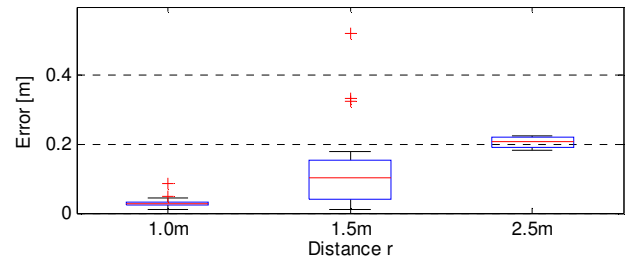


Fig. 5: Boxplot of errors dependent on distance

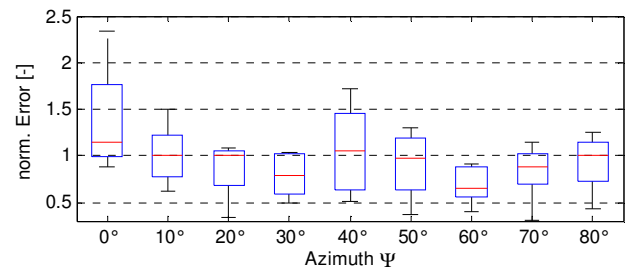


Fig. 6: Boxplot of normalised errors dependent on azimuth angle

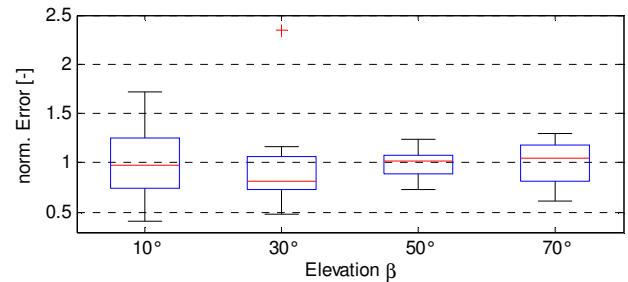


Fig. 7: Boxplot of normalised errors dependent on elevation angle

The results within groups (e)-(g), belonging to a distance of 1.5 m, show much more disturbance. The means of error are in the range of 100 mm, what is not surprising, but four outliers went through the sanity check. These outliers are based on images with one marker detection only. This is where the sanity check is not effective. Furthermore, the outliers are based on very few samples within the 100 images for the position in question. Many of the 510 images without detections mentioned above

can be found amongst these images. In group (e) and (f) only small markers could be detected, this reasons the bad performance of the system within these groups. Errors in group (g) are obviously smaller than in (e) and (f). Due to bigger elevation the larger marker is detectable here, which leads to reduced errors. The visibility of the larger marker is very dependent on its illumination. Figure 2 (bottom line) gives an impression of illumination changing with elevation.

Figure 5 gives a detailed view on distance dependency of estimation errors. The boxplot indicates the median value by a red line, the range from first to third quartile by a blue box and the most extreme values by a black bar. Outliers are plotted by red crosses but neglected for the boxes. Median error values are 30 mm for 1.0 m distance, 100 mm for 1.5 m distance and 210 mm for 2.5 m distance. Errors could be expected to increase with increasing distance as the position estimation depends on the estimated orientation. Influence of the errors in orientation on errors in position are weighted by distance to the reference array.

To evaluate the influence of azimuth angles on accuracy, all errors belonging to one group were normalised and rearranged according to azimuth angle. The result is shown with help of a boxplot in figure 6. Errors rise gently, if the viewing direction is rectangular to one of the small markers horizontal directions. In general the influence of azimuth angle is very minor.

To evaluate the influence of elevation, the same analysis was done regarding elevation angles. The analysis was limited to distances of 1.0 m, as for the other distances elevation was not varied in the entire range. Figure 7 shows the associated results. No significant influence of elevation is noticeable. But, as seen above, the elevation has influence on errors at longer distances.

4.3 Discussion of results

Compared to the requirements formulated in chapter 3 – errors in position less than 150 mm – it can be stated, that the implemented system shows a general suitability for tracking small

UAVs during precision landing. The overall accuracy is sufficient for landing on the designated platform. The inherent conical reduction of errors in position while approximating the landing platform is well suited for the precision landing problem. The errors gets smaller the closer the UAV is getting towards the landing platform.

The unreliable position estimation in medium or larger distances in conjunction with low elevations is acceptable, as long as the UAV maintains a minimal approach angle. Nevertheless, additional mid-sized markers might improve the system.

Data of the performed accuracy evaluation can be used to improve usage of the position estimates of the system. As a typical example a Kalman filter updated by data of the optical tracking system could be mentioned. The filter could adjust the weighting of the tracking system's estimated position dependent on the distance to the marker array.

All measurements were carried out in a static test setup. Thus, data on performance during flight is missing. There are several influences that could downgrade the system's performance in flight. First flight tests showed a slightly degraded image quality due to vibrations and vehicle movements. On the other hand the position estimations remained reasonable during flight test.

5 Conclusion

In this paper a navigation approach for vertical precision landing using optical tracking has been presented. For this purpose a new concept, a spatial array of retroreflective markers on the landing platform, has been proposed. A static measurement series to evaluate accuracy during landing has been carried out.

Results of these system tests have shown a general applicability of the approach for precision landing in context of the ANCHORS project. In particular the inherent conical reduction of errors in position while approaching the platform is well suited for the landing problem. The retroreflective marker coating enabled the system to work in varying ambient light as well as in complete darkness.

To improve the system's dynamics during landing, the influence of the processing speed of multiple marker detections should be investigated in future in more detail. Towards application of the presented approach on board an UAV in an outdoor environment, future work should put more effort on a detailed quantitative evaluation of all accuracy and reliability related effects for vehicle specific landing trajectories.

Acknowledgment

Our work has been conducted within the ANCHORS (UAVAssisted Ad Hoc Networks for Crisis Management and Hostile Environment Sensing, 13N12204) project. This project is funded by the German Federal Ministry of Education and Research (BMBF) and Agence Nationale Recherche (ANR) in the context of the Franco-German call "Cooperation in Civil Security research between Germany and France". We thank all project partners for their work and contributions to the ANCHORS project.



Contact

P. Hartmann hartmann@fsd.rwth-aachen.de

References

- [1] International Atomic Energy Agency, *International fact finding expert mission of the Fukushima Daiichi NPP accident following the great east-Japan earthquake and tsunami*, Japan, 2011, p.139
- [2] Nemeč, B. Robot Grasping Using an ArToolKit Library *Elektrotehniški vestnik*, Vol. 77, No. 1 2010, pp. 69-74
- [3] Kato H, Billinghurst M, Marker tracking and HMD calibration for a video-based augmented reality conferencing system *Proc 2nd IEEE and ACM International Workshop on Augmented Reality*, San Francisco, pp. 85-94, 1999

- [4] Barfield W, Caudell T. *Fundamentals of Wearable Computers and Augmented Reality* Erlbaum Associates Inc. Hillsdale, NJ, 2000
- [5] Wagner D, Reitmayr G, Mulloni A, Drummond T, Schmalstieg D. Pose tracking from natural features on mobile phones *Proc International Symposium on Mixed and Augmented Reality*, Cambridge, 2008, pp. 125-134
- [6] Xiang Z, Fronz S, Navab N. Visual marker detection and decoding in AR systems: a comparative study *Proc International Symposium on Mixed and Augmented Reality*, 2002, pp. 97-106
- [7] Pentenrieder K, Meier P, Klinker G. Analysis of Tracking Accuracy for Single-Camera Square-Marker-Based Tracking, *Proc Third Workshop on Virtual and Augmented Reality of the GI-Fachgruppe VR/AR*, Koblenz, Germany, September, 2006
- [8] Masselli A, Zell A. A Novel Marker Based Tracking Method for Position and Attitude Control of MAVs *Proc International Micro Air Vehicle Conference and Flight Competition*, Braunschweig, Germany, 2012, pp. 1-6
- [9] Ducard G, D'Andrea R. Autonomous Quadrotor Flight Using a Vision System and Accommodating Frames Misalignment. *Proc IEEE International Symposium on Industrial Embedded Systems*, 2009
- [10] Cassinis R, Tampalini F F, Fedrigotti R. Active markers for outdoor and indoor robot localization *Proc DEA-Unibs*, 2005
- [11] Lupashin S, Hehn M, Mueller M W, Schoellig A P, Sherback M, D'Andrea R. A platform for aerial robotics research and demonstration: The Flying Machine Arena, *Mechatronics*, Vol. 24, Issue 1, February 2014, pp. 41-54
- [12] Wagner D, Schmalstieg D. ARToolKitPlus for Pose Tracking on Mobile Devices *Proc 12th Computer Vision Winter Workshop*, 2007

Copyright Statement

The authors confirm that they, and/or their company or organization, hold copyright on all of the original material included in this paper. The authors also confirm that they have obtained permission, from the copyright holder of any third party material included in this paper, to publish it as part of their paper. The authors confirm that they give permission, or have obtained permission from the copyright holder of this paper, for the publication and distribution of this paper as part of the ICAS 2014 proceedings or as individual off-prints from the proceedings.